

01 Jan 2023

Dispatching Point Selection For A Drone-based Delivery System Operating In A Mixed Euclidean–Manhattan Grid

Francesco Betti Sorbelli

Federico Corò

Sajal K. Das

Missouri University of Science and Technology, sdas@mst.edu

Cristina M. Pinotti

et. al. For a complete list of authors, see https://scholarsmine.mst.edu/comsci_facwork/1350

Follow this and additional works at: https://scholarsmine.mst.edu/comsci_facwork

 Part of the [Computer Sciences Commons](#)

Recommended Citation

F. Betti Sorbelli et al., "Dispatching Point Selection For A Drone-based Delivery System Operating In A Mixed Euclidean–Manhattan Grid," *Annals of Operations Research*, Springer, Jan 2023.
The definitive version is available at <https://doi.org/10.1007/s10479-023-05458-4>

This Article - Journal is brought to you for free and open access by Scholars' Mine. It has been accepted for inclusion in Computer Science Faculty Research & Creative Works by an authorized administrator of Scholars' Mine. This work is protected by U. S. Copyright Law. Unauthorized use including reproduction for redistribution requires the permission of the copyright holder. For more information, please contact scholarsmine@mst.edu.



Dispatching point selection for a drone-based delivery system operating in a mixed Euclidean–Manhattan grid

Francesco Betti Sorbelli¹ · Federico Corò¹ · Sajal K. Das² · Cristina M. Pinotti¹ · Anil Shende³

Accepted: 6 June 2023
© The Author(s) 2023

Abstract

In this paper, we present a drone-based delivery system that assumes to deal with a mixed-area, i.e., two areas, one rural and one urban, placed side-by-side. In the mixed-areas, called EM-grids, the distances are measured with two different metrics, and the shortest path between two destinations concatenates the Euclidean and Manhattan metrics. Due to payload constraints, the drone serves a single customer at a time returning back to the dispatching point (DP) after each delivery to load a new parcel for the next customer. In this paper, we present the 1-Median Euclidean–Manhattan grid Problem (MEMP) for EM-grids, whose goal is to determine the drone's DP position that minimizes the sum of the distances between all the locations to be served and the point itself. We study the MEMP on two different scenarios, i.e., one in which all the customers in the area need to be served (full-grid) and another one where only a subset of these must be served (partial-grid). For the full-grid scenario we devise optimal and approximation algorithms, while for the partial-grid scenario we devise an optimal algorithm.

Keywords Drone · Delivery system · Logistics · Facility location · Euclidean and Manhattan metrics

✉ Federico Corò
federico.coro@unipg.it
Francesco Betti Sorbelli
francesco.bettisorbelli@unipg.it
Sajal K. Das
sdas@mst.edu
Cristina M. Pinotti
cristina.pinotti@unipg.it
Anil Shende
shende@roanoke.edu

¹ Department of Mathematics and Computer Science, University of Perugia, 06123 Perugia, Italy

² Department of Computer Science, Missouri University of Science and Technology, Rolla, MO 65401, USA

³ Department of Mathematics, Computer Science and Physics, Roanoke College, Salem, VA 24153, USA

1 Introduction

Drones or Unmanned Aerial Vehicles (UAVs) are recently becoming widely used in civil applications such as environmental protection (Calamoneri et al., 2022; Justin et al., 2022; Qu et al., 2023; Wivou et al., 2016), public safety (He et al., 2017; Li et al., 2015; Pant et al., 2021), localization (Niculescu et al., 2022), and smart agriculture (Jawad et al., 2019; Moribe et al., 2018). Currently, there is a growing interest in the use of drones in smart cities (Nguyen & Nguyen, 2021). This interest is particularly increased after the global presence of the COVID-19 disease (Jat & Singh, 2020; Preethika et al., 2020). Recently, (Anggraeni et al., 2020) discuss about the use of drones as carriers for distributing and transporting drugs and medicines, and revealed that 86.7% of people agree that drones are more effective, surely faster, and less polluting than any ground-based distribution system. Quarantine, closure of borders, and social distancing forced people to stay indoors for long periods, allowing them to go out only for essential activities. Therefore, considering the need to avoid all unnecessary direct human contact, people started to rely heavily on online stores for their regular shopping. In parallel, large companies like Amazon are testing drone-based delivery systems, particularly for what is known as “last-mile” small item logistics. For example, Amazon introduced “Amazon Air Prime”, a service that uses drones able to deliver goods up to 25 kg to customers within a radius of 16 km (Pandit & Poojari, 2014; Shavarani et al., 2018; Welch, 2015), and Domino’s developed a pizza-delivery service using drones (Pepitone, 2013).

There are countless advantages to using drones for deliveries, including economic benefits, saving on greenhouse gas, and the ability to deliver in time-critical situations or hard-to-reach places. With the growth of commercial interest, researchers have begun to study variants of the Traveling Salesman Problem (TSP) for drones (Ha et al., 2015). However, due to the payload constraint that forces the drone to return after each delivery, TSP is not suitable for drones (Dayarian et al., 2020; Sawadsitang et al., 2019). Of particular interest is the work proposed by Agatz et al. (2018), where a drone combined with a truck is used to make multiple deliveries in a given area, going back and forth from the truck. In that case, it is crucial to find the best location for the truck, to minimize the distance traveled by the drone.

In this article, we imagine offering a drone delivery service to the customers of a delivery area that covers a mixed-area, i.e., two areas, one rural and one urban, placed side-by-side. In urban areas, for safety and privacy reasons (see regulation of inhabited centers, e.g., FAA 2023), it is assumed that the drone flies over the streets since it cannot fly beyond a certain maximum allowed altitude. Namely, in urban areas, it might be forbidden for the drone to travel along the straight line connecting the dispatching point and the delivery if such a straight line, due to tall obstacles, exists only at an altitude higher than the maximum altitude allowed by the regulations. However, the drone can at least save time—if not distance traveled—in the urban area. In fact, a drone is usually faster than a conventional wheeled vehicle in a crowded area: it will certainly not get stuck in traffic. In rural areas, instead, due to the fact that tall buildings are not present, the drone can move freely and follow the shortest path to reach its destination, making clear its advantage on the traveled distance in this case. In the case of mixed areas, i.e., rural and urban areas placed side-by-side, the drone must follow both the Euclidean and Manhattan metrics.

We model the proposed drone delivery area as a two-dimensional mixed-grid. The vertices of the grid represent both the possible locations of the drone’s DP and the possible delivery destinations, and they are placed in rows and columns as in a regular 2-D grid. To model the two different types of areas through which the drone can move, we have divided the

grid into two parts: the rural area and the urban area. In the former, the distance between two destinations respects the Euclidean metric, while in the latter, the metric is Manhattan (taxicab geometry). We are then interested in finding where to set the DP, i.e., the truck location from where the drone starts, in order to minimize the sum of the distances between a subset of delivery destinations and the DP itself. Due to strict payload constraints, the drone must return back to the DP after each delivery. Therefore, the drone needs to travel back and forth from the DP as many times as the number of delivery destinations on the grid. In this paper, we consider two delivery scenarios. The full-grid scenario where each point of the grid has to be served by the drone. In light of the COVID-19 pandemic, this scenario happens, for example, if the drone is used to deliver meals in a lockdown area, or to deliver self-tests to sick people. In this particular example, the full-grid scenario is also justified by the fact that after every delivery the drone should be properly sanitized and disinfected before performing the next delivery, as proposed by Kunovjanek and Wankmüller (2021). The partial-grid scenario, instead, assumes that only a subset of points of the grid is a delivery site. This is the usual scenario in a delivery system.

The DP selection problem in logistics, while sharing similarities with the classical facility location problem, requires a more complex modeling approach that considers factors such as varying demand and transportation costs, and it involves optimizing multiple metrics simultaneously (Euclidean and Manhattan), which is not the case for the original facility location problem.

In this paper, we present extensions and improvements to our earlier work discussed in two conference papers, i.e., Bartoli et al. (2019) and Betti Sorbelli et al. (2019). In Bartoli et al. (2019) we focused on the full-grid scenario. In this paper we extend our work to include a partial-grid scenario. We suitably adapt results and ideas from Betti Sorbelli et al. (2019) to this scenario, and provide new efficient algorithms for both the scenarios. The contributions of this paper are summarized as follows.

- We introduce the EM-grid model, which characterizes the delivery area for the drone, formed by two contiguous areas, i.e., one rural and one urban, that follow the Euclidean and Manhattan metrics, respectively.
- We define the 1-Median Euclidean–Manhattan grid Problem (MEMP) and devise time-efficient algorithms for the full-grid and partial-grid scenarios. For the full-grid scenario we devise optimal and approximation algorithms, while for the partial-grid scenario we devise an optimal algorithm. We also give all the proofs for the full-grid scenario that had been left blank in the previous conference paper (Bartoli et al., 2019).

The rest of the paper is organized as follows. Section 2 reviews the related work. Section 3 formally defines MEMP. Sections 4 and 5 describe properties and algorithms for efficiently solving MEMP with full-grid and partial-grid scenarios, respectively. Finally, Sect. 6 offers conclusions and future research directions.

2 Related work

In the literature, many works attempt to solve the drone-based last-mile delivery problem. To the best of our knowledge, drones have been considered in a delivery system for the first time by Murray and Chu (2015). Specifically, they study the cooperation between a truck and a drone to deliver packages to customers. The problem to solve is the Flying Sidekick Traveling Salesman Problem (FSTSP), which is a variant of the classic TSP. In the FSTSP, a drone can autonomously perform deliveries to the customers directly flying from the main

depot or can be helped by a truck. In the latter case, the drone flies from the truck, delivers the package, and then rendezvouses with the truck again in a third location. However, when the drone flies, the truck can do other deliveries independently, but still, it has to wait for the drone at the rendezvous location. For solving FSTSP, the authors propose an optimal mixed-integer linear programming (MILP) and two heuristics for solving instances of practical sizes. Then, Murray and Raj (2020) investigate the same scenario with multiple drones in by introducing the Multiple Flying Sidekicks Traveling Salesman Problem (mFSTSP). Even for the mFSTSP, they provide an optimal MILP formulation along with a heuristic solution approach that consists of solving a sequence of three sub-problems.

Recently, Dell'Amico et al. (2022) present an exact formulation for FSTSP while also simplifying the model reducing the number of constraints and thus be able to solve several benchmark instances from the literature.

However, in these works, the drones fly according to the Euclidean metric. Kloster et al. (2023) introduce the multiple Traveling Salesman Problem with Drone Stations (mTSP-DS), which is an extension to the classical multiple Traveling Salesman Problem (mTSP). In this problem, multiple trucks starting to/from a single depot are in charge of supplying some packet stations that host autonomous vehicles (drones or robots). On these stations, each truck can launch and operate drones/robots to serve customers. The objective of mTSP-DS is to serve all customers minimizing the makespan. The problem is formulated as an MILP only suitable to solve small instances. For larger instances, many matheuristic algorithms are presented. Schermer et al. (2019) introduce the Vehicle Routing Problem with Drones and En Route Operations (VRPDERO), which is an extension to the Vehicle Routing Problem with Drones (VRPD). In this problem, drones may not only be launched and retrieved at vertices but also on some discrete points that are located on each arc. The problem is formulated as an MILP, and matheuristic approaches are presented to deal with large instances. The goal of both (Schermer et al., 2019; Kloster et al., 2023) is to minimize the makespan, while ours is to find the best DPs from where to launch the drones.

Bartoli et al. (2019) introduce the drone-based delivery area modeled as EM-grids where a drone is used for delivering small packages to customers. Given the delivery area divided into two contiguous areas, i.e., the rural and the urban areas, the goal is to find the optimal DP (depot or warehouse) for the drone in order to minimize the sum of all the distances between all the potential customers and the DP itself. However, due to strict payload constraints, the drone cannot serve more than a customer at a time, and after each delivery, the drone must go back to the depot. A similar approach, but in a different context, has been studied by Betti Sorbelli et al. (2019). In such a scenario, the objective is to determine the optimal cart point for the drone that minimizes the distances between a set of items (on shelves) and the cart itself, assuming that shelves follow the two aforementioned metrics. Differently from Bartoli et al. (2019), in Betti Sorbelli et al. (2019) only a subset of points needs to be considered. Moreover, Betti Sorbelli et al. (2019) compare the current human-based system with respect to the newly proposed one based on drones.

Brown et al. (2021) compare and contrast the performance of many algorithms in a delivery scenario. They model the delivery area as a circular region with a central depot, while customers are randomly distributed throughout the region. Different temporal and spatial metrics are compared when evaluating these algorithms. In particular, they evaluate the impact of having distances measured according to both the Euclidean and Manhattan distance metrics. The number of customers stochastically varies under both Manhattan and Euclidean distance metrics. The paper states that the number of customer deliveries and the metric used to measure travel distance impacts a decision maker's choice of the best algorithm and that employing multiple algorithms is recommended.

Ai et al. (2021) explore the implications and advantages of strategic planning on urban delivery services. More specifically, the preferred method and local impacts of vehicle trips may vary by neighborhood characteristics (e.g., traffic or customer demands). Instead of searching for an optimal route, the paper focuses on the estimation of the vehicles' miles traveled (VMT) per meal order, considering different types of neighborhoods, delivery scenarios, and strategies. The proposed system is tested and evaluated in Chicago, showing that alternative delivery strategies can greatly reduce the VMT per order based on the type of neighborhood. In the evaluation, both the Euclidean and Manhattan metrics are combined. However, although different metrics have been evaluated, drones have not been used in either Brown et al. (2021) or Ai et al. (2021).

Recently, there has been more effort in solving the last-mile delivery problem using drones instead of a standard vehicle, due to the flexibility of drones and their capability to fly over obstacles and avoid traffic. Poikonen et al. (2019) investigate the problem of solving the TSP with a Drone (TSP-D) where the drone rides on the truck.

Betti Sorbelli et al. (2022) investigate the cooperation between a truck and multiple drones. Each delivery is characterized by a drone's energy cost, a reward based on its priority, and a time interval (launch and rendezvous with the truck). This work aims at finding an optimal scheduling for the drones that maximizes the overall reward, subject to the drone's battery capacity while ensuring that the same drone performs deliveries that do not overlap. Results show that the presented problem is NP -hard, therefore, different heuristics for solving the problem in a time-efficient way are proposed. More recently, Betti Sorbelli et al. (2023) investigate the feasibility of performing deliveries with a drone in the presence of external factors such as wind.

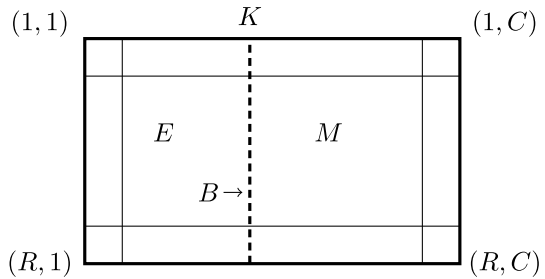
Li et al. (2020) compare the traditional truck-based delivery system against the drone-based one to reduce the general energy consumption and hence reduce the gas emissions. They also take into account traffic congestion. They propose a mixed-integer green routing model with traffic restrictions and a genetic algorithm to efficiently solve the complex routing problem, showing that drones can accomplish more deliveries and at a lower cost (in terms of CO_2 emissions and energy consumption) compared to standard methods and that traffic types impact the results.

Salama and Srinivas (2020) study the last-mile scenario formed by multiple drones assisted by a single truck that carries them. The customers to be served by the drones form a clustering, and each drone is assigned to a specific cluster. The initial position of a drone is called a "cluster focal point". Once all the focal points are computed, the truck needs to visit these points by minimizing its traveled route. Moreover, due to payload constraints, the drones serve their customers one at a time. The truck cannot follow the Euclidean metric, while the drones do. The authors propose an optimal mixed integer nonlinear programming (MINLP) solution as well as an unsupervised machine learning-based heuristic algorithm.

Dukkanci et al. (2021) present a variation on the theme. The proposed model assumes that drones are assisted by trucks, that carry them through the city. The trucks start from the main depot and park the drones in specific locations where drones have to serve the customers by a sequence of back-and-forth flights. Both the trucks and the drones move according to the Euclidean metric. The introduced problem is called Energy Minimizing and Range Constrained Drone Delivery Problem (ERDDP) whose objective is to minimize the total operational cost including an explicit calculation of the energy consumption of the drone as a function of the drone's speed. The ERDDP is formulated as a second order cone program instance.

Pinto and Lagorio (2022) propose a last-mile drone delivery scenario where multiple drones can exploit charging stations to replenish their batteries. In this setting, the drones can

Fig. 1 The EM-grid: E models the rural area, while M models the urban area



fly from the main hub to the terminal station and serve, one at a time, a subset of customers in the neighborhood, and then go back to the hub. Alternatively, they can move from a terminal station to a charging station to refill the battery and perform subsequent deliveries to other neighborhoods belonging to other terminal stations. The objective function aims to either minimize the number of charging stations or to minimize the overall traveled distance. The authors solve this problem by proposing an optimal and a heuristic solution.

Karak and Abdelghany (2019) combine the pickup and the delivery requests in a system with stations (nodes in a given graph) and introduce the Hybrid Vehicle-Drone Routing Problem. Vehicles visit stations to transport delivery items and drones, while drones are launched and collected only at stations. The problem is formulated as a mixed-integer program, which minimizes the vehicle and drone routing cost to serve all customers. To solve the problem, the authors use an extension of the classic Clarke and Wright algorithm (see Clarke and Wright 1964), a known heuristic to solve the Vehicle Routing Problem. We remark that while their goal is to find the best route for drones and trucks, our goal is to find the best stations, i.e., the DPs, from where to launch the drones.

Finally, Hong et al. (2018) investigate the problem of placing drone charging facilities in an area to help increase the coverage range of drones for commercial deliveries. The authors present an MILP formulation, and then a heuristic is proposed to effectively solve the problem.

3 Problem definition

In this section, we first introduce the delivery area model and how the drone moves inside it, and then formally describe the problem to solve. We model the mixed-area where the deliveries occur as two areas, one rural and one urban, placed side-by-side.

3.1 Delivery area model

We define the *Euclidean–Manhattan-Grid* (EM-grid) as $G = (R, C, K)$, that is a 2-D grid with R rows, C columns, and the *Border* B is the column $K \in [1, C]$ that separates the *Euclidean* grid E (rural area) from the *Manhattan* grid M (urban area) (see Fig. 1). Specifically, $E = \{1, \dots, R\} \times \{1, \dots, K\}$, $B = \{1, \dots, R\} \times \{K\} \subseteq E$, and $M = \{1, \dots, R\} \times \{K + 1, \dots, C\}$.

We assume that the drone delivery system covers a rectangular area: E and M have the same number of rows R . The border consists of a single column, i.e., K . Conventionally, the area consists only of a rural area region if $K = C$ (i.e., $M = \emptyset$), whereas it is effectively limited

to an urban area if $K = 1$. In an EM-grid, there are vertices and edges connecting adjacent vertices. Any internal vertex $u = (r_u, c_u)$ of G , i.e., with $1 < r_u < R$ and $1 < c_u < C$, is connected to the four adjacent vertices $(r_u, c_u \pm 1)$ and $(r_u \pm 1, c_u)$; whereas, in general, any vertex of the grid, i.e., with $1 \leq r_u \leq R$ and $1 \leq c_u \leq C$, is connected only to the existing adjacent vertices (i.e., an external vertex has only three or two neighbors). For simplicity, we assume that the distance between any two pairs of consecutive vertices on the same row or column is constant and unitary, and so the *weight* of any edge is unitary. In this work, the “distance” is a measure of the *time required* for performing the delivery, or of the *needed energy* for shipping the package. We also assume that every customer can be reached by the drone to/from the *dispatching point* (DP). The DP can be a permanent or non-permanent location inside the delivery area that is used by drones for serving customers. We imagine that before any delivery instance, a truck (or any other vehicle) brings all the goods/packages at the DP along with a drone so that the drone can start delivering packages. We used this definition because it is broader, and can be used to denote both the points returned by the OPT-P and OPT-F algorithms. At the DP, the drone can recharge its battery, or just replace it with fresh ones. Let $\bar{R} = \lceil \frac{R}{2} \rceil$ be the middle row, let $\bar{C} = \lceil \frac{C}{2} \rceil$ be the middle column, and let $\bar{K} = \lceil \frac{K}{2} \rceil$ be the column that halves the Euclidean sub-grid.

For any two vertices u, v in G , the distance $d(u, v)$ is the length of the shortest path traversed by the drone in the EM-grid to go from vertex u to the destination v . The Euclidean and Manhattan distances are defined, respectively, as $d_E(u, v) = \sqrt{(r_u - r_v)^2 + (c_u - c_v)^2}$ and $d_M(u, v) = |r_u - r_v| + |c_u - c_v|$.

We note that the shortest path between a vertex $u \in E$ and a vertex $v \in M$ is given by $\min_{w \in B} \{d_E(u, w) + d_M(w, v)\}$. In Lemma 1 we prove that such path is unique and passes through the vertex on the border B that has the same row as v .

Lemma 1 Consider an EM-Grid $G = (R, C, K)$. Given $u = (r_u, c_u) \in E$ and $v = (r_v, c_v) \in M$, then $d(u, v) = d_E(u, h) + d_M(h, v)$ with $h = (r_v, K)$.

Proof Consider the vertex $h = (r_v, K)$ which shares the same row as v , and another vertex $w = (i, K)$ in B with $h \neq w$. We want to prove that: $d_E(u, h) + d_M(h, v) \leq d_E(u, w) + d_M(w, v)$. This follows by the triangle inequality applied to the vertices u, w, h , i.e., $d_E(u, h) \leq d_E(u, w) + |r_v - i| = d_E(u, w) + d_M(w, h)$. \square

Thus, from now on, $d(u, v)$ is given by:

$$d(u, v) = \begin{cases} d_E(u, v) & \text{if } u, v \in E \\ d_M(u, v) & \text{if } u, v \in (M \cup B) \\ d_E(u, h) + d_M(h, v) & \text{if } u \in E, v \in M \text{ where } h = (r_v, K) \in B \\ d_M(u, h) + d_E(h, v) & \text{if } u \in M, v \in E \text{ where } h = (r_u, K) \in B \end{cases} \quad (1)$$

3.2 The column-cost

Let the *column-cost* be the distance traversed by the drone starting from a vertex u in the middle-row \bar{R} to serve all the vertices of a given column, where the column is on the same side (Euclidean or Manhattan) of the grid as the vertex u . Such column-cost depends on which side of the grid the column and the vertex u reside and on the number of rows R . Let $\Delta_E(j)$ be the column-cost to serve a Euclidean column at distance j from the candidate DP $u = (\bar{R}, c_u)$ with $u \in E$. Similarly, let $\Delta_M(j)$ be the column-cost to serve a Manhattan

column at distance j from the drone's DP $u = (\bar{R}, c_u)$ with $u \in M \cup B$. One can easily find that:

$$\Delta_E(j) = j + 2 \sum_{i=1}^{\bar{R}-1} \sqrt{i^2 + j^2} + ((R-1) \bmod 2) \sqrt{\bar{R}^2 + j^2} \quad (2)$$

$$\begin{aligned} \Delta_M(j) &= j + 2 \sum_{i=1}^{\bar{R}-1} (i+j) + ((R-1) \bmod 2) (\bar{R}+j) \\ &= \bar{R}(\bar{R}+1+2j) + j + ((R-1) \bmod 2)(\bar{R}+j) \end{aligned} \quad (3)$$

3.3 The problem formulation

In our scenario, the fundamental task is to serve, with the aid of a drone, the customers of an area, e.g., to distribute viral tests to potentially infected patients. Due to payload constraints (and, e.g., to avoid the spread of the disease), the drone cannot serve all the customers on the same flight, and it has necessarily to go back and forth from a specific position inside the delivery area (called DP, where the drone, e.g., can be also sanitized each time) to all the customers. Specifically, this DP is the point in which all the products for customers are initially stored. Hence, the objective is to minimize the distance traveled by the drone when it moves inside the delivery area. We denote this problem as the 1-Median Euclidean–Manhattan grid Problem (MEMP) since the goal is to find a *single* DP inside EM-grids.

Given an EM-grid $G = (R, C, K)$ and a subset of vertices $H \subseteq G$, for an arbitrary vertex $u = (r_u, c_u) \in G$, we define the cost of delivery from u to each point in H , denoted by $\mathcal{C}(H, u)$, as:

$$\mathcal{C}(H, u) = 2 \sum_{v \in H} d(v, u) \quad (4)$$

As noted above, the distance between points u and v is a measure of the cost of delivery from u to v , and the multiplicative constant 2 is in consideration of the round trip for each delivery. Given $H \subseteq G$, let H_E and H_M be the subset of points that lie in the Euclidean and Manhattan grid, respectively, such that $H_E \cup H_M = H$ and $H_E \cap H_M = \emptyset$. The set H is formed by $n = |H|$ vertices, where $n_E = |H_E|$ and $n_M = |H_M|$, such that $n = n_E + n_M$.

When $H = G$, Eq. (4) can be rewritten as:

$$\mathcal{C}(G, u) = 2 \sum_{v \in G} d(v, u) = 2 \sum_{r_v=1}^R \sum_{c_v=1}^C d((r_v, c_v), u) \quad (5)$$

with $v = (r_v, c_v) \in G$, and $r_v \in [1, R]$ and $c_v \in [1, C]$. We refer to the scenario as a *partial-grid scenario* (respectively, *full-grid scenario*) when $H \subset G$ (respectively, $H = G$). Finally, given $H \subseteq G$, we define the DP (median) u^* as:

$$u^* = \arg \min_{u=(r_u, c_u) \in G} \mathcal{C}(H, u) \quad (6)$$

4 Solving MEMP with full-grid scenario

In this section we give properties and then devise algorithms for solving MEMP for the full-grid scenario. This full-grid scenario is justified by the fact that a delivery company

Table 1 Comparison between the algorithms that solve MEMP in the full-grid scenario

DP	Algorithm	Section	Time complexity	Approximation ratio
u^*	OPT-F	4.2	$\mathcal{O}(\log K)$	1
u_M	CMALL-F	4.3.1	$\mathcal{O}(1)$	$\sqrt{2}$

has to consider all the grid's locations as potential customers. For example, in the case of a quarantined area, as with COVID-19, the drone can be used to deliver goods of primary necessity to all the residents in the area. Therefore, the objective would be to find the optimal location to set the DP in order to minimize the travel distances between any customer's locations and the DP.

In the following, we first discuss how to optimally solve MEMP with a full-grid (see Sect. 4.2), and then we propose an approximation algorithm, CMALL-F, that operates as if the grid is a full Manhattan grid (i.e., $K = 0$) and provides a guaranteed approximation bound of $\sqrt{2}$ (see Sect. 4.3.1).

In Table 1 we compare the presented algorithms that solve MEMP in the full-grid scenario evaluating their time complexities and guaranteed approximation bounds. In particular, Table 1 reports the DP computed by the algorithm (second column) along with the time complexity (without including the preprocessing phase time).

4.1 Properties

In the following we prove some properties that we will exploit to devise our optimal algorithm. We first note that with a full Manhattan grid (i.e., $K = 1$) or a full Euclidean grid (i.e., $K = C$), MEMP can be trivially solved. In the former case, MEMP has the Manhattan-median in $u^* = (R, C)$ (see Yamaguchi and Kaji 1987). Note that, the median is not unique when the values C and R are even. In the latter case, by using symmetry arguments, it can be proven that MEMP has the Euclidean-median in $u^* = (\bar{R}, \bar{C})$. For the general case when $1 < K < C$, we can derive properties to narrow down the set of possible median point candidates.

First, we observe that the median always belongs to the middle row \bar{R} of G .

Theorem 1 *Given an EM-grid $G = (R, C, K)$, the median $u^* = (r^*, c^*)$ satisfies $r^* = \bar{R}$.*

Proof Let the row-cost $\Gamma(u, h)$ be the distance traversed by a drone with DP $u = (r_u, c_u)$ to serve all the vertices on a row at distance h from u . Note that the function Γ depends only on the relative distance between the first coordinate r_u of u and the row considered. There are potentially two rows at distance h from u : one above u at row $r_u + h$, and one below u at row $r_u - h$. The crucial observation is that the two rows have exactly the same row cost when served by u . For a fixed u , $\Gamma(u, h)$ increases with h . In other words, for $h_2 > h_1$, it holds that $\Gamma(u, h_2) - \Gamma(u, h_1) > 0$.

Now we can show that u^* belongs to row \bar{R} , proving that for a given $u = (\bar{R}, z)$ and $v = (\ell, z)$, with $\ell \neq \bar{R}$, it holds $\mathcal{C}(G, u) \leq \mathcal{C}(G, v)$. First, we consider $\ell > \bar{R}$. In this case:

$$\mathcal{C}(G, u) = 2 \sum_{x=1}^{\bar{R}-1} \Gamma(u, x) + \Gamma(u, 0) \quad (7)$$

$$\mathcal{C}(G, v) = \sum_{x=1}^{\ell-1} \Gamma(v, x) + \sum_{x=1}^{n-\ell} \Gamma(v, x) + \Gamma(v, 0) \quad (8)$$

Subtracting $\mathcal{C}(G, u)$ from $\mathcal{C}(G, v)$, one has:

$$\sum_{x=\bar{R}}^{\ell-1} \Gamma(u, x) - \sum_{w=n-\ell+1}^{\bar{R}-1} \Gamma(u, w) \geq 0 \quad (9)$$

In Eq. (9) $x \geq \bar{R}$, while $w < \bar{R}$, and accordingly it holds $\Gamma(u, x) \geq \Gamma(u, w)$. Hence $\mathcal{C}(G, u) \leq \mathcal{C}(G, v)$ for any v . Similarly, the result can be proven when $\ell < \bar{R}$. \square

Recall the notion of *column-cost* defined in Sect. 3.2. Recall, also, that $n = |G|$. Algebraically the following properties can be proven about the column-cost:

Lemma 2 1. Both $\Delta_E(j)$ and $\Delta_M(j)$ increase with j ;

2. $\Delta_M(j) - \Delta_M(j-t) = t \cdot n$ for $j \geq t$;

3. $\Delta_E(j) - \Delta_E(j-t)$ is positive and strictly monotone increasing with j for all $j > t$;

4. $\Delta_E(j) - \Delta_E(j-t) \geq t(\Delta_E(j-t+1) - \Delta_E(j-t))$, $\Delta_E(j) - \Delta_E(j-t) \leq t(\Delta_E(j) - \Delta_E(j-1))$;

5. $\Delta_E(j) < \Delta_M(j) \leq \sqrt{2}\Delta_E(j)$.

Proof We prove each point separately:

1. Let $j_1 > j_2$. From Eq. (2), it holds $\sqrt{i^2 + j_1^2} > \sqrt{i^2 + j_2^2}$. From Eq. (3), it holds $i + j_1 > i + j_2$.
2. From Eq. (3), it holds $t + 2(\bar{R} - 1)t = tn$.
3. From Eq. (2), it holds $\sqrt{i^2 + j^2} > \sqrt{i^2 + (j-t)^2}$. Now, differentiating with respect to j one obtains:

$$1/\sqrt{(i/j)^2 + 1} - 1/\sqrt{(i/(j-t))^2 + 1}.$$

Since $t > 0$, $j > j - t$, and hence $\frac{i}{j-t} > \frac{i}{j}$, confirming the strictly monotone increase for $j > t$.

4. Observe that $\Delta_E(j) - \Delta_E(j-t)$ can be rewritten as the sum of the distance of consecutive columns as $\sum_{z=0}^{t-1} \Delta_E(j-z) - \Delta_E(j-z-1)$. By applying Property 2 with $t = 1$, it holds $\Delta_E(j) - \Delta_E(j-t) \geq t(\Delta_E(j-t+1) - \Delta_E(j-t))$ because $\Delta_E(j-z) - \Delta_E(j-z-1)$ is increasing with $j-z$. Similarly, it follows: $\Delta_E(j) - \Delta_E(j-t) \leq t(\Delta_E(j) - \Delta_E(j-1))$.
5. Recalling the well-known Cauchy-Schwarz inequality $\sqrt{a^2 + b^2} < (a + b) \leq \sqrt{2}\sqrt{a^2 + b^2}$, it holds: $\Delta_E(j) < \Delta_M(j) \leq \sqrt{2}\Delta_E(j)$. \square

Having established in Theorem 1 that u^* is on the row \bar{R} , the potential candidates for the median are vertices (\bar{R}, c) . For a vertex that belongs to the middle row, say (\bar{R}, c) , let $\bar{\mathcal{C}}(c) = \mathcal{C}(G, c)$. Selecting an arbitrary vertex $u = (\bar{R}, c_u)$ as the candidate median, we can exploit the column-cost definition and decompose the cost $\bar{\mathcal{C}}(c_u)$ into C_1, \dots, C_4 as defined in Eqs. (10a) and (10b). Both equations coincide when $c_u = K$ because $\Delta_M(0) = \Delta_E(0)$ and $\Delta_M(0) + iR = \Delta_M(i)$.

$$\bar{C}(c_u) \left\{ \begin{array}{l} \text{if } c_u \in E \\ \underbrace{\sum_{j=0}^{c_u-1} \Delta_E(j)}_{C_1=\text{cost}(E)} + \underbrace{\sum_{j=1}^{K-c_u} \Delta_E(j) + (C-K)\Delta_E(K-c_u) + R \sum_{j=1}^{C-K} j}_{C_2=\text{cost}(M)} \quad (10a) \\ \\ \text{if } c_u \in M \cup B \\ \underbrace{\sum_{j=1}^K \Delta_E(j) + R(K-1)(c_u-K)}_{C_3=\text{cost}(E-B)} + \underbrace{\sum_{j=0}^{c_u-K} \Delta_M(j) + \sum_{j=1}^{C-c_u} \Delta_M(j)}_{C_4=\text{cost}(M \cup B)} \quad (10b) \end{array} \right.$$

We now prove some technical results to help to further reduce the set of median candidates. We first show, in Lemma 3, that the median cannot be “too close” to the left border of G .

Lemma 3 *The column c^* of the DP $u^* = (\bar{R}, c^*)$ of $G = (R, C, K)$ cannot be in the interval $[1, \dots, \bar{K} - 1]$, where $\bar{K} = \lceil \frac{K}{2} \rceil$ is the column that halves the Euclidean sub-grid.*

Proof This is equivalent to saying that, if $c_u \in [1, \bar{K} - 1]$, then $\bar{C}(c_u) > \bar{C}(\lfloor \frac{K}{2} \rfloor)$.

From Eq. (10a), we notice that the cost C_1 increases if $c_u < \bar{K}$ because c_u is a sub-optimal solution for the median of the Euclidean sub-grid in G . Namely, \bar{K} is the median of an EM-grid $G' = (R, K, K)$. Moreover, by Lemma 2 (Property 2), the cost $(C - K)\Delta_E(K - c_u) > (C - K)\Delta_E(\bar{K})$ because $K - c_u > \bar{K}$. \square

Next, we show, in Lemma 4 that $\bar{C}(c_u)$ is convex when c_u varies from \bar{K} to K .

Lemma 4 *Varying c_u from \bar{K} to K , the delivery cost function $\bar{C}(c_u)$ has a single minimum.*

Proof Let t , with $\bar{K} \leq t \leq K - 1$, be the vertex where the delivery cost assumes the first minimum. Therefore from Eq. (10a) we have that:

$$\begin{aligned} \bar{C}(t+1) - \bar{C}(t) &= \Delta_E(t+1) - \Delta_E(K-t) \\ &\quad + (C-K)(\Delta_E(K-(t+1)) - \Delta_E(K-t)) \geq 0 \end{aligned} \quad (11)$$

To prove that the cost function has exactly one minimum in the interval $[\bar{K}, \dots, K]$, it is sufficient to show that $\bar{C}(t+2) - \bar{C}(t+1) \geq 0$ given that $\bar{C}(t+1) - \bar{C}(t) \geq 0$.

First, observe by Lemma 2 (Property 2) that:

$$\Delta_E(K-(t+2)) - \Delta_E(K-(t+1)) \geq \Delta_E(K-(t+1)) - \Delta_E(K-t) \quad (12)$$

Then,

$$\begin{aligned} \bar{C}(t+2) - \bar{C}(t+1) &= \Delta_E(t+2) - \Delta_E(K-(t+1)) \\ &\quad + (C-K)(\Delta_E(K-(t+2)) - \Delta_E(K-(t+1))) \\ &\geq \Delta_E(t+2) - \Delta_E(K-(t+1)) \\ &\quad + (C-K)(\Delta_E(K-(t+1)) - \Delta_E(K-t)) \\ &= \underbrace{\Delta_E(t+2) - \Delta_E(t+1)}_{\geq 0} + \underbrace{\Delta_E(K-t) - \Delta_E(K-(t+1))}_{\geq 0} \end{aligned} \quad (13)$$

$$+ \bar{C}(t+1) - \bar{C}(t) \geq \bar{C}(t+1) - \bar{C}(t) \geq 0 \quad (14)$$

\square

So, we know now that the optimal column cannot be in the interval $[1, \dots, \bar{K} - 1]$, and that $\bar{C}(c_u)$ has a single minimum in the interval $[\bar{K}, K]$. We can have two cases here: $K \leq \bar{C}$ and $K > \bar{C}$. Lemma 5 shows that when $K \leq \bar{C}$, there is only one vertex candidate as the median on the Manhattan side, while Lemma 6 establishes the fact that when $K > \bar{C}$, the median cannot be in $[\bar{C}, C]$.

Lemma 5 *Let $K \leq \bar{C}$. Varying c_u in the Manhattan side, $K \leq c_u \leq C$, the delivery cost function $\bar{C}(c_u)$ has a single minimum in \bar{C} .*

Proof Since the candidate median is on the Manhattan side, the delivery cost is expressed by Eq. (10b). Moving the candidate from (\bar{R}, c_u) to $(\bar{R}, c_u + 1)$, the vertices on the left of c_u (including c_u itself) increase by exactly one their distance from the median. Whereas, the vertices on the right of the column c_u decrease their distance from the median by one. Hence, the delivery cost function decreases as long as $K \leq c_u \leq \bar{C}$. \square

Lemma 6 *Let $K > \bar{C}$. The value of the median candidate column cannot be greater than \bar{C} .*

Proof We can first exclude any candidate with $c_u \geq K$ because, as we seen in Lemma 5, the delivery cost function $\bar{C}(c_u)$ is increasing for $c_u \geq K$. Moreover, in order to exclude the candidates in the range $[\bar{C}, K]$, we first prove that $\bar{C}(\bar{C} + 1) > \bar{C}(\bar{C})$. Namely,

$$\begin{aligned} \bar{C}(\bar{C} + 1) - \bar{C}(\bar{C}) &= \Delta_E(\bar{C} + 1) - \Delta_E(K - \bar{C}) \\ &\quad - (C - 1 - K) (\Delta_E(K - \bar{C}) - \Delta_E(K - (\bar{C} + 1))) \geq 0 \end{aligned} \quad (15)$$

because, by Property 2) and 2) of Lemma 2

$$\begin{aligned} \Delta_E(\bar{C} + 1) - \Delta_E(K - \bar{C}) &> (2\bar{C} + 1 - K) (\Delta_E(K - \bar{C} + 1) - \Delta_E(K - \bar{C})) \\ &> (2\bar{C} + 1 - K) (\Delta_E(K - \bar{C}) - \Delta_E(K - \bar{C} - 1)) \\ &\geq (C - 1 - K) (\Delta_E(K - \bar{C}) - \Delta_E(K - (\bar{C} + 1))) \end{aligned} \quad (16)$$

Since we have proven in Lemma 4 that if the cost function is increasing in one vertex of row \bar{R} , then it is increasing in all the vertices on its right, there are no candidates for the median greater than \bar{C} . \square

Then, Theorem 2 follows immediately from Theorem 1, and Lemmas 3, 5, and 6.

Theorem 2 *Suppose $u^* = (r^*, c^*)$ be the median for $G = (R, C, K)$. Let $c, \bar{K} \leq c \leq K$ be such that*

$$\bar{C}(c) = \min_{i \in [\bar{K}, K]} \{\bar{C}(i)\}$$

and, let $c', \bar{K} \leq c' \leq \bar{C}$ be such that

$$\bar{C}(c') = \min_{i \in [\bar{K}, \bar{C}]} \{\bar{C}(i)\}$$

Then, $r^ = \bar{R}$, and*

$$c^* = \begin{cases} c & \text{if } K \leq \bar{C} \text{ and } \bar{C}(c) < \bar{C}(\bar{C}) \\ \bar{C} & \text{if } K \leq \bar{C} \text{ and } \bar{C}(c) \geq \bar{C}(\bar{C}) \\ c' & \text{otherwise} \end{cases}$$

\square

4.2 The optimal algorithm OPT-F

Theorem 2 directly translates to algorithm OPT-F (see the pseudo-code in Algorithm 1) that optimally solves MEMP in the full-grid scenario.

Algorithm 1 The OPT-F Algorithm

```

1: if  $K \leq \bar{C}$  then
2:    $c \leftarrow \text{find-minimum}(\bar{K}, K)$ 
3:   if  $\bar{C}(c) < \bar{C}(\bar{C})$  then
4:     return  $(\bar{R}, c)$  ▷ see Lemma 4
5:   else
6:     return  $(\bar{R}, \bar{C})$  ▷ see Lemma 5
7:   end if
8: else
9:    $c \leftarrow \text{find-minimum}(\bar{K}, \bar{C})$  ▷ see Lemma 6
10:  return  $(\bar{R}, c)$ 
11: end if

```

Given a closed interval of column numbers, the procedure `find-minimum` returns the column number, c , in that interval such that the total delivery cost from the DP (\bar{R}, c) is the least over all the vertices (\bar{R}, i) for i in the given closed interval.

4.2.1 Time complexity of algorithm OPT-F

Note that the minimum in $[\bar{K}, K]$, returned by invoking the procedure `find-minimum`, can be found by applying a binary search due to the unimodality proven in Lemma 4. Similarly, when $K > \bar{C}$ (Line 8), the minimum is in the interval $[\bar{K}, \bar{C}]$, i.e., a sub-interval of $[\bar{K}, K]$. Thus, as above, it can be found through the `find-minimum` procedure in Line 9. The time complexity of the `find-minimum` procedure is logarithmic in the width of the sub-interval where the minimum resides. The interval has a width of $\frac{K}{2}$ in Line 2, and a width of $\frac{C}{2} - \frac{K}{2} \leq K - \frac{K}{2} = \frac{K}{2}$ in Line 9 since $K \geq \frac{C}{2}$. Thus, we can conclude that, in each case, the time complexity of `find-minimum` is $\mathcal{O}(\log K)$.

With regards to the time complexity of the OPT-F algorithm, we observe that for a fixed c_u , the delivery cost $\bar{C}(c_u)$ can be computed in $\mathcal{O}(1)$ time by applying Eq. (10a) if the prefix sums of the column-cost are computed in a pre-processing phase. The column-costs $\Delta_E(j)$ and their prefix sums $\sum_{t=1}^j \Delta_E(t)$, for $1 \leq j \leq K$, can be computed and memorized in a vector in $\mathcal{O}(RK + K)$ time. For $1 \leq j \leq K$, the K column-costs $\Delta_M(j)$ and their prefix sums $\sum_{t=1}^j \Delta_M(t)$ can be computed and memorized in a vector in $\mathcal{O}(K)$ time by using the closed-form in Eq. (3). Then, assuming that the prefix-sums of the column-costs are given as input to the algorithm, i.e., they are computed in a pre-processing phase, each $\bar{C}(c_u)$ can be computed in constant time. Thus, the optimal point u^* can be computed by the OPT-F algorithm in $\mathcal{O}(\log K)$ time.

4.3 Approximation algorithms

In the previous section, we presented an algorithm that optimally solves MEMP in the full-grid scenario, taking logarithmic time in the number of columns of the grid. In this section,

Table 2 Comparison between the algorithms that solve MEMP in the partial-grid scenario

DP	Algorithm	Section	Time complexity	Approximation ratio
$u_{\hat{C}}$	CEMB-P	5.2	$\mathcal{O}(nR \log K)$	—
$u_{\hat{M}}$	CMEB-P	5.3	$\mathcal{O}(nR)$	—
u^*	OPT-P	5.4	$\mathcal{O}(nR \log K)$	1

we present the CMALL-F algorithm for solving MEMP in the full-grid scenario. We also establish an upper bound on the approximation ratio for algorithm CMALL-F.

4.3.1 Algorithm CMALL-F

Algorithm CMALL-F returns the Manhattan-median $u_M = (\bar{R}, \bar{C})$ as the DP. That is, CMALL-F operates as if the grid is a full Manhattan grid (i.e., $K = 1$). This algorithm is sub-optimal for $1 < K < C$ providing a guaranteed approximation bound of $\sqrt{2}$, while it is optimal when $K = 1$ or $K = C$.

Lemma 7 *The CMALL-F algorithm provides a $\sqrt{2}$ approximation ratio when $1 < K < C$.*

Proof Let u^* be the median for $G = (R, C, K)$. Since the Euclidean column-cost $\Delta_E(j)$ is smaller than the Manhattan column-cost $\Delta_M(j)$, $\mathcal{C}(G, u_M) \leq \mathcal{C}_M(G, u_M)$, where $\mathcal{C}_M(G, u_M)$ is the cost when $K = 1$. Moreover, $\mathcal{C}(G, u^*) > \mathcal{C}_E(G, u^*)$ because the Manhattan distance is at least as much as the Euclidean distance. Then, $\mathcal{C}_E(G, u^*) > \mathcal{C}_E(G, u_M)$ because u_M is the Euclidean-median of $G = (R, C, C)$. Thus, by the Cauchy–Schwarz inequality in Lemma 2:

$$\frac{\mathcal{C}(G, u_M)}{\mathcal{C}(G, u^*)} < \frac{\mathcal{C}_M(G, u_M)}{\mathcal{C}_E(G, u_M)} \leq \sqrt{2}.$$

The CMALL-F algorithm finds the point u_M in constant time, so its time complexity is $\mathcal{O}(1)$. \square

5 Solving MEMP with partial-grid scenario

In this section, we focus on MEMP in the partial-grid scenario. In this case, we are given $H \subset G$ as the n delivery points, i.e., $|H| = n$.

We first discuss the trivial cases where $K = 1$, i.e., a full Manhattan grid, and $K = C$, i.e., a full Euclidean grid (see Sect. 5.1). The rest of the sections deals with the general cases.

In Sects. 5.2 and 5.3 we propose two heuristic algorithms, CEMB-P and CMEB-P, assuming the optimal DP is in the Euclidean side of the grid, and in the Manhattan side of the grid, respectively. Note that neither of these two algorithms returns the optimal DP. Algorithm CEMB-P returns the best DP candidate in E , whereas CMEB-P returns the best DP candidate in M .

Then, in Sect. 5.4 we combine the above two heuristic algorithms and present algorithm OPT-P to find the optimal median, the DP, in G .

To summarize the above, we tabulate in Table 2 the presented algorithms that solve MEMP in the partial-grid scenario along with their time complexities and guaranteed approximation bounds.

5.1 Special cases

We first discuss how to optimally solve MEMP to serve a subset of customers on a grid that is not mixed, i.e., either Manhattan or Euclidean. In a Manhattan grid (i.e., an EM-grid with $K = 1$), given a subset $H \subset G$ of customers, MEMP with partial-grid scenario can be trivially solved in $\mathcal{O}(|H|)$ time by selecting $u^* = (r_{u^*}, c_{u^*})$ where r_{u^*} is the median of the row coordinate of the customers and c_{u^*} is the median of the column coordinate of the customers (see Yamaguchi and Kaji 1987).

In the literature, there are many results concerning the problem, called *geometric median*, of determining the DP that minimizes the sum of distances between the points of a given set $H \subset \mathbb{R}^d$ and the DP itself. The geometric median is denoted as the Euclidean-median in two-dimensional space.

Although the Euclidean-median is unique and the sum $\mathcal{C}(H, u)$ of the distances from each customer to the DP u is positive and strictly convex in \mathbb{R}^d , as proven by Vardi and Zhang (2000), there is no exact and closed expression for the Euclidean-median of an arbitrary set H of real points.

In a Euclidean grid (i.e., an EM-grid with $K = C$), MEMP with partial-grid scenario can be solved more easily because the candidate positions in the plane are just the vertices of G , and the number of attempts to determine the single Euclidean-median is limited by the fact that EM-grid is formed by R rows and C columns. So, a trivial solution for MEMP with partial-grid takes $\mathcal{O}(RC|H|)$ time because for each position u of the grid the cost $\mathcal{C}(H, u)$ can be computed in time $\mathcal{O}(|H|)$. Exploiting the fact that, in \mathbb{R}^2 , $\mathcal{C}(H, u)$ is positive and strictly convex when u moves on a single row of the grid, the position in a row that provides the minimum cost $\mathcal{C}(H, u)$ can be computed by a slightly modified binary search. So, MEMP with a subset of customers on a Euclidean grid can be solved in $\mathcal{O}(R \log C|H|)$ time because for each row of the grid only $\log C$ candidates are tested.

In the next section, for the general case, i.e., the mixed-grid with $1 < K < C$, we leverage the observation that the median u^* resides either in M or in E .

5.2 The CEMB-P algorithm

Algorithm CEMB-P solves MEMP assuming that $u^* \in E$, i.e., the optimal DP is in the Euclidean side of the grid, and returns (and forces) $u_{\hat{C}} \in E$ selecting as the DP the point in the Euclidean side E that minimizes the overall traveling cost.

For any DP $u \in E$, by Lemma 1, for each point v in H_M (the subset of H that contains the vertices in the Manhattan side), the drone must travel horizontally from the border B to v . So, the drone covers the same fixed cost in the Manhattan grid regardless of the position of $u \in E$. This motivates our algorithm whose pseudo-code is presented in Algorithm 2.

We construct the multi-set H'_M consisting of the projections of all the points in H_M to the border B (Algorithm 2, Line 1). Then, we compute the point $u_{\hat{C}} \in E$ that minimizes the sum of the distances to the points in the multi-set $H' = H_E \cup H'_M$, taking into account the multiplicity of points in H' . Towards this, for each row (Algorithm 2, Line 3) we evaluate the minimum from the first to the K^{th} column, and update the overall minimum, if necessary. By exploiting the fact that in the Euclidean space the function $\mathcal{C}(H, u)$ to minimize is positive and strictly convex (see Vardi and Zhang 2000), we know that $\mathcal{C}(H, u)$ is unimodal when fixing a row and varying the columns. Hence, we can calculate the minimum on each row by performing a time-efficient binary search that requires logarithmic time (Algorithm 2, Line 4).

Since the cost of movement in M does not change the minimum, the returned value, $u_{\hat{C}}$, is the best DP in E .

Algorithm 2 The CEMB-P Algorithm

```

1:  $H'_M \leftarrow \{(r_u, K) \in B \mid u \in H_M\}$ ,  $H' \leftarrow H_E \cup H'_M$ 
2:  $u_{\hat{C}} \leftarrow \emptyset$ ,  $cost \leftarrow +\infty$ 
3: for  $i \in 1, \dots, R$  do
4:    $u_i^* \leftarrow \text{find-minimum-on-row}(i, H', 1, K)$ 
5:   if  $C(H', u_i^*) < cost$  then
6:      $u_{\hat{C}} \leftarrow u_i^*$ ,  $cost \leftarrow C(H', u_i^*)$ 
7:   end if
8: end for
9: return  $u_{\hat{C}}$ 

```

About the time complexity, due to the fact that there are n points to serve, and since we perform R binary searches (one for each row of a Euclidean grid with K columns), the total cost of CEMB-P is $\mathcal{O}(nR \log K)$.

5.3 The CMEB-P algorithm

Algorithm CMEB-P solves MEMP assuming that $u^* \in M$, i.e., the optimal DP is in the Manhattan side of the grid, and returns (and forces) $u_{\hat{M}} \in M$ selecting as the DP the point in the Manhattan side M that minimizes the overall traveling cost.

For any DP, u in M , by Lemma 1, the drone has to fly through the projection of $u \in B$ to serve any point of H_E . Thus, for any DP u , there is one intermediate point in B for all drone paths from u to points in H_E . Note that the intermediate point does not depend on the column c_u of the DP u . This motivates our algorithm whose pseudo-code is presented in Algorithm 3.

We first compute the column median, χ , of the points in H' , consisting of the points in H_M and the points in H_E moved to the border. The function `column-median` takes into account the possible multiplicity of points in H' . Since we are only concerned with the column numbers, we can move each point in H_E to any point on the border; we move all of them to $(1, K)$ (Algorithm 3, Lines 2 and 3).

Since the median in M can reside in R different rows, we have R candidate intermediate points, which are the points of the border B . For each row i , we construct the multi-set $H'_E(i)$ consisting of all the points in H_E moved to the intermediate point (i, K) on the border B (Algorithm 3, Line 5). We then consider the point $u_i^* = (i, \chi) \in M$ as the median of the points in the multi-set $H' = H_M \cup H'_E(i)$.

With u_i^* as the DP, the cost of delivery is the sum of two costs: (1) the cost of flying the drone between u_i^* and each point in H' , with all distances calculated according to the Manhattan metric, and (2) the cost of flying the drone between each point in H_E and the intermediate point corresponding to u_i^* , with all distances calculated according to the Euclidean metric (Algorithm 3, Line 8).

The algorithm returns as $u_{\hat{M}}$ the intermediate point that witnesses the least cost, over all the possible intermediate points, and is thus the best DP in M .

As for the complexity of the algorithm, we compute the column median of n points once. Then, for every row i , the cost $cost(H_E \rightarrow (i, K))$ has to be computed, and this requires $\mathcal{O}(|H_E|)$ time.

Algorithm 3 The CMEB-P Algorithm

```

1:  $u_{\hat{M}} \leftarrow \emptyset, c \leftarrow +\infty$ 
2:  $H'_E(1) \leftarrow \{(r_u, 1) \in B \mid u \in H_E\}, H' \leftarrow H'_E(1) \cup H_M$ 
3:  $\chi \leftarrow \text{column-median}(H')$ 
4: for  $i \in 1, \dots, R$  do
5:    $H'_E(i) \leftarrow \{(r_u, i) \in B \mid u \in H_E\}, H' \leftarrow H'_E(i) \cup H_M$ 
6:    $u_i^* \leftarrow (i, \chi)$ 
7:    $C_i \leftarrow \mathcal{C}(H', u_i^*) + \text{cost}(H_E \rightarrow (i, K))$ 
8:   if  $C_i < c$  then
9:      $u_{\hat{M}} \leftarrow u_i^*$ 
10:     $c \leftarrow C_i$ 
11:   end if
12: end for
13: return  $u_{\hat{M}}$ 

```

Thus, the algorithm's complexity is $\mathcal{O}(n + R|H_E|)$.

5.4 The optimal OPT-P algorithm

Having computed the best DPs on both sides of EM-grid we can now optimally solve MEMP with partial-grid scenario.

The OPT-P algorithm finds the optimal point u^* by comparing the best point between $u_{\hat{C}}$ and $u_{\hat{M}}$. Given that Algorithm CEMB-P returns the best DP in E , and Algorithm CMEB-P returns the best DP in M , the simple idea of OPT-P is to compare these two points and return the best one, as follows:

$$u^* = \arg \min \{\mathcal{C}(H, u_{\hat{C}}), \mathcal{C}(H, u_{\hat{M}})\}. \quad (17)$$

About the time complexity, recalling that CEMB-P takes $\mathcal{O}(nR \log K)$ and CMEB-P takes $\mathcal{O}(nR)$, the overall time complexity of OPT-P is $\mathcal{O}(nR \log K)$.

6 Conclusion

We considered a drone-based delivery system for the “last-mile” logistics of small parcels, medicines, or viral tests, in EM-grids. The shortest path in an EM-grid concatenates Euclidean and Manhattan distances. We solved the MEMP on EM-grids whose goal is to minimize the sum of the distances between the locations to be served and the drone's DP. Finding the most suitable DP has many implications that can impact the expected delivery time for customers, the energy consumption of drones, and in general, the broader environmental impacts, e.g., the quantity of CO₂ emissions, when relying on trucks. We propose efficient algorithms to exactly solve the problem in EM-grids in both the full-grid and the partial-grid scenarios under the assumption that the vertex distance is unitary.

In future work, we intend to extend the introduced mixed-grid model to more general layouts (e.g., a rural (green) area inside an urban area like Central Park in New York). Nevertheless, we believe that our work could be the starting point to devising much more complex scenarios to better model real-world scenarios. For example, we could a map extraction technique to construct a grid, G , where the each individual grid square is labeled as “Buildings” or “Park”. A contiguous group of squares labeled “Buildings” is effectively a Manhattan

grid, and a contiguous group of squares labeled “Park” is a Euclidean grid. Then, we could sub-divide G into multiple EM-grids, and apply our algorithms suitably in each EM-grid.

Another interesting variant to study is the use of multiple drones that are responsible for delivering packages to different partitions of the customers. In this case, we will need efficient clustering algorithms for minimizing suitable metrics.

Author Contributions All the authors contributed equally to the paper.

Funding Open access funding provided by Università degli Studi di Perugia within the CRUI-CARE Agreement. This work was supported in part by the “GNCS – INdAM”, and by “RESIDUAL UniPG”. The work of S. K. Das was partially supported by the NSF SIRAC project (Smart Integrated Farm Network for Agricultural Communities) under Award No. 1952045.

Data availability The manuscript has no associated data.

Declarations

Competing Interests The authors have no relevant financial or non-financial interests to disclose.

Ethical approval This article does not contain any studies with human participants or animals performed by any of the authors.

Open Access This article is licensed under a Creative Commons Attribution 4.0 International License, which permits use, sharing, adaptation, distribution and reproduction in any medium or format, as long as you give appropriate credit to the original author(s) and the source, provide a link to the Creative Commons licence, and indicate if changes were made. The images or other third party material in this article are included in the article's Creative Commons licence, unless indicated otherwise in a credit line to the material. If material is not included in the article's Creative Commons licence and your intended use is not permitted by statutory regulation or exceeds the permitted use, you will need to obtain permission directly from the copyright holder. To view a copy of this licence, visit <http://creativecommons.org/licenses/by/4.0/>.

References

- Agatz, N., Bouman, P., & Schmidt, M. (2018). Optimization approaches for the traveling salesman problem with drone. *Transportation Science*. <https://doi.org/10.1287/trsc.2017.0791>
- Ai, N., Zheng, J., Chen, X., & Kawamura, K. (2021). Neighborhood-specific traffic impact analysis of restaurant meal delivery trips: Planning implications and case studies in Chicago. *Journal of Urban Planning and Development*, 147(2), 05021013.
- Anggraeni, S., Maulidina, A., Dewi, M. W., Rahmadiani, S., Rizky, Y. P. C., Arinalhaq, Z. F., Usdiyana, D., Nandiyanto, A. B. D., Al-Obaidi, A. S., et al. (2020). The deployment of drones in sending drugs and patient blood samples covid-19. *Indonesian Journal of Science and Technology*. <https://doi.org/10.17509/ijost.v5i2.24462>
- Bartoli, L., Betti Sorbelli, F., Corò, F., Pinotti, C. M., & Shende, A. (2019). Exact and approximate drone warehouse for a mixed landscape delivery system. In *International Conference on Smart Computing (SMARTCOMP)* (pp. 266–273). IEEE.
- Betti Sorbelli, F., Corò, F., Das, S. K., Palazzetti, L., & Pinotti, C. M. (2022). On the scheduling of conflictual deliveries in a last-mile delivery scenario with truck-carried drones. *Pervasive and Mobile Computing*, 87, 101700.
- Betti Sorbelli, F., Corò, F., Palazzetti, L., Pinotti, C. M., & Rigoni, G. (2023). How the wind can be leveraged for saving energy in a truck-drone delivery system. *IEEE Transactions on Intelligent Transportation Systems*, 24, 4038–4049.
- Betti Sorbelli, F., Corò, F., Pinotti, C. M., & Shende, A. (2019). Automated picking system employing a drone. In *International Conference on Distributed Computing in Sensor Systems (DCOSS)* (pp. 633–640). IEEE.
- Brown, J. R., Bushuev, M. A., & Guiffrida, A. L. (2021). Distance metrics matter: Analysing optimisation algorithms for the last mile problem. *Journal of Logistics Systems and Management*, 38(2), 151–174.

- Calamoneri, T., Corò, F., & Mancini, S. (2022). A realistic model to support rescue operations after an earthquake via UAVs. *IEEE Access*, 10, 6109–6125.
- Clarke, G., & Wright, J. W. (1964). Scheduling of vehicles from a central depot to a number of delivery points. *Operations Research*, 12(4), 568–581.
- Dayarian, I., Savelsbergh, M., & Clarke, J.-P. (2020). Same-day delivery with drone resupply. *Transportation Science*, 54(1), 229–249.
- Dell'Amico, M., Montemanni, R., & Novellani, S. (2022). Exact models for the flying sidekick traveling salesman problem. *International Transactions in Operational Research*, 29(3), 1360–1393.
- Dukkanci, O., Kara, B. Y., & Bektaş, T. (2021). Minimizing energy and cost in range-limited drone deliveries with speed optimization. *Transportation Research. Part C: Emerging Technologies*, 125, 102985.
- FAA. (2023). Faadronzone. <https://faadronzone.faa.gov>. Accessed on May 2023.
- Ha, Q. M., Deville, Y., Pham, Q. D., & Hà, M. H. (2015). Heuristic methods for the traveling salesman problem with drone. *Journal of Scientific Computing*.
- He, D., Chan, S., & Guizani, M. (2017). Drone-assisted public safety networks: The security aspect. *IEEE Communications Magazine*, 55(8), 218–223.
- Hong, I., Kuby, M., & Murray, A. T. (2018). A range-restricted recharging station coverage model for drone delivery service planning. *Transportation Research. Part C: Emerging Technologies*, 90, 198–212.
- Jat, D. S., & Singh, C. (2020). Artificial intelligence-enabled robotic drones for covid-19 outbreak. In A. Joshi, N. Dey, & K. C. Santosh (Eds.), *Intelligent systems and methods to combat covid-19* (pp. 37–46). Singapore: Springer.
- Jawad, A. M., Jawad, H. M., Nordin, R., Gharghan, S. K., Abdullah, N. F., & Abu-Alshaeer, M. J. (2019). Wireless power transfer with magnetic resonator coupling and sleep/active strategy for a drone charging station in smart agriculture. *IEEE Access*, 7, 139839–139851.
- Justin, C. Y., Payan, A. P., & Mavris, D. N. (2022). Integrated fleet assignment and scheduling for environmentally friendly electrified regional air mobility. *Transportation Research Part C: Emerging Technologies*, 138, 103567.
- Karak, A., & Abdelghany, K. (2019). The hybrid vehicle-drone routing problem for pick-up and delivery services. *Transportation Research Part C: Emerging Technologies*, 102, 427–449.
- Kloster, K., Moeini, M., Vigo, D., & Wendt, O. (2023). The multiple traveling salesman problem in presence of drone-and robot-supported packet stations. *European Journal of Operational Research*, 305(2), 630–643.
- Kunovjanek, M., & Wankmüller, C. (2021). Containing the covid-19 pandemic with drones-feasibility of a drone enabled back-up transport system. *Transport Policy*, 106, 141–152.
- Li, X., Guo, D., Yin, H., & Wei, G. (2015). Drone-assisted public safety wireless broadband network. In *2015 IEEE wireless communications and networking conference* (pp. 323–328). IEEE.
- Li, Y., Yang, W., & Huang, B. (2020). Impact of UAV delivery on sustainability and costs under traffic restrictions. *Mathematical Problems in Engineering*. <https://doi.org/10.1155/2020/9437605>
- Moribe, T., Okada, H., Kobayashi, K., & Katayama, M. (2018). Combination of a wireless sensor network and drone using infrared thermometers for smart agriculture. In *2018 15th IEEE annual consumer communications & networking conference (CCNC)* (pp. 1–2). IEEE.
- Murray, C. C., & Chu, A. G. (2015). The flying sidekick traveling salesman problem: Optimization of drone-assisted parcel delivery. *Transportation Research. Part C: Emerging Technologies*, 54, 86–109.
- Murray, C. C., & Raj, R. (2020). The multiple flying sidekicks traveling salesman problem: Parcel delivery with multiple drones. *Transportation Research. Part C: Emerging Technologies*, 110, 368–398.
- Nguyen, H. P. D., & Nguyen, D. D. (2021). Drone application in smart cities: The general overview of security vulnerabilities and countermeasures for data communication. In R. Krishnamurthi, A. Nayyar, & A. E. Hassanien (Eds.), *Development and future of internet of drones* (pp. 185–210). Cham: Springer.
- Niculescu, V., Palossi, D., Magno, M., & Benini, L. (2022). Energy-efficient, precise UWB-based 3-D localization of sensor nodes with a nano-UAV. *IEEE Internet of Things Journal*, 10, 5760–5777.
- Pandit, V., & Poojari, A. (2014). A study on amazon prime air for feasibility and profitability: A graphical data analysis. *IOSR Journal of Business and Management*, 16(11), 06–11.
- Pant, Y. V., Li, M. Z., Rodionova, A., Quaye, R. A., Abbas, H., Ryerson, M. S., & Mangharam, R. (2021). FADS: A framework for autonomous drone safety using temporal logic-based trajectory planning. *Transportation Research Part C: Emerging Technologies*, 130, 103275.
- Pepitone, J. (2013). Domino's tests drone pizza delivery. *CNNMoney*, June, 4.
- Pinto, R., & Lagorio, A. (2022). Point-to-point drone-based delivery network design with intermediate charging stations. *Transportation Research. Part C: Emerging Technologies*, 135, 103506.
- Poikonen, S., Golden, B., & Wasil, E. A. (2019). A branch-and-bound approach to the traveling salesman problem with a drone. *INFORMS Journal on Computing*, 31(2), 335–346.
- Preethika, T., Vaishnavi, P., Agnishwar, J., Padmanathan, K., Umashankar, S., Annapoorani, S., Subash, M., & Aruloli, K. (2020). Artificial intelligence and drones to combat covid-19. Preprints.

- Qu, C., Betti Sorbelli, F., Singh, R., Calyam, P., & Das, S. K. (2023). Environmentally-aware and energy-efficient multi-drone coordination and networking for disaster response. *IEEE Transactions on Network and Service Management*. <https://doi.org/10.1109/TNSM.2023.3243543>
- Salama, M., & Srinivas, S. (2020). Joint optimization of customer location clustering and drone-based routing for last-mile deliveries. *Transportation Research. Part C: Emerging Technologies*, 114, 620–642.
- Sawadsitang, S., Niyato, D., Tan, P. S., Wang, P., & Nutanong, S. (2019). Multi-objective optimization for drone delivery. In *90th vehicular technical conference (VTC2019-Fall)* (pp. 1–5). IEEE.
- Schermer, D., Moeini, M., & Wendt, O. (2019). A hybrid VNS/Tabu search algorithm for solving the vehicle routing problem with drones and en route operations. *Computers & Operations Research*, 109, 134–158.
- Shavarani, S. M., Nejad, M. G., Rismanchian, F., & Izbirak, G. (2018). Application of hierarchical facility location problem for optimization of a drone delivery system: A case study of amazon prime air in the city of san francisco. *The International Journal of Advanced Manufacturing Technology*, 95, 3141–3153.
- Vardi, Y., & Zhang, C.-H. (2000). The multivariate l1-median and associated data depth. *Proceedings of the National Academy of Sciences*, 97(4), 1423–1426.
- Welch, A. (2015). A cost-benefit analysis of amazon prime air.
- Wivou, J., Udawatta, L., Alshehhi, A., Alzaabi, E., Albeloshi, A., & Alfalasi, S. (2016). Air quality monitoring for sustainable systems via drone based tech. In *International conference on information and automation for sustainability (ICIAfS)*, (pp. 1–5). IEEE.
- Yamaguchi, T., & Kaji, I. (1987). Some location problems on grid graphs. *Electronics and Communications in Japan (Part I: Communications)*, 70(10), 31–40.

Publisher's Note Springer Nature remains neutral with regard to jurisdictional claims in published maps and institutional affiliations.